Original Research

Calliandra portoricensis ameliorates ovarian and uterine oxido-inflammatory responses in *N*-methyl-*N*-nitrosourea and benzo[a]pyrene-treated rats

Adedoyin O Adefisan[1], Judith C Madu[1], Solomon E Owumi[2] (ID) and Oluwatosin A Adaramoye[1] (ID)

[1]Molecular Drug Metabolism and Toxicology Laboratories, Faculty of Basic Medical Sciences, College of Medicine, University of Ibadan, Ibadan 200005, Nigeria; [2]Cancer Research and Molecular Biology Laboratories, Department of Biochemistry, Faculty of Basic Medical Sciences, College of Medicine, University of Ibadan, Ibadan 200005, Nigeria
Corresponding author: Solomon E Owumi. Email: zicri@hotmail.com

Impact statement

Infertility resulting from reproductive impairment is traumatic in families. Exposure to chemicals may play insidious roles not easily connected to infertility. We examined benzo[a]pyrene (BaP), and *N*-methyl nitrosourea (NMU)-induced ovarian and uterine toxicity and the role of *Calliandra portoricensis* in mitigating toxicity. In a bid to illuminate folk medical claims cloaked in mystery, unearthing lost knowledge, advance natural chemopreventive agents, and report new evidence lacking in the literature attributed to *CP*. Although *CP* is known to exhibit anticonvulsant, antidiarrheal, antipyretic, antirheumatic, and analgesic effects in humans, its possible roles for mitigating toxicity stemming from inadvertent chemical exposures are reported here. Our findings affirm and further show that *CP* abates toxic response incumbent on oxidative damage and inflammatory responses associated with NMU and BaP exposure. Development of phytochemical derived from *CP* may serve as a potential natural therapy against chemical toxicities in individuals inadvertently exposed, and promote human health and reproductive satiety.

Abstract

Reproductive dysfunction stemming from chemical agents may lead to infertility. We examined the protective effects of *Calliandra portoricensis* (*CP*) extract on benzo[a]pyrene (BaP) and *N*-methyl-*N*-nitrosourea (NMU)-induced ovarian and uterine toxicity in rat, treated as follows: control (group 1), NMU + BaP (group 2), groups 3 and 4 received (NMU + BaP), and *CP* (50 and 100 mg/kg), respectively. Group 5: *CP* (100 mg/kg) alone, group 6: (NMU + BaP) and vincristine (VIN: 0.5 mg/kg) and group 7: VIN alone. Rats were injected at age 7, 10, and 13 weeks with single doses of NMU and BaP for 10 consecutive weeks. NMU + BaP significantly ($P < 0.05$) increased ovarian and uterine weight, and decreased bodyweight, while the organo-somatic index (OSI) of uterus and ovary increased 2.3 and 1.4 folds, respectively. *CP* co-treatment ameliorated the observed weight changes. Lipid peroxidation increased by 58% in the ovary, accompanied by decreases in ovarian and uterine GST, GPx, catalase activities, and total sulfhydryl level in NMU + BaP-treated rats. Uterine and ovarian myeloperoxidase activities, as well as nitric oxide levels also increased. *CP* co-treatment ameliorated the observed changes in antioxidant enzymes and inflammatory biomarkers. Furthermore, histopathology revealed fibrotic ovarian stroma, while uterine endometrium was infiltrated with inflamed cells. Immunohistochemistry showed weak expression of FSH, LH, p53, caspase-3, and Bax, whereas progesterone, iNOS, and Bcl-2 were strongly expressed in NMU + BaP-treated rats. *CP* treatment restored the architecture of these tissues. Conclusively, the root bark fraction of *CP* decreases oxido-inflammatory damage in ovarian and uterine tissues of NMU- and BaP-treated rats.

Keywords: *Calliandra portoricensis*, *N*-methyl-*N*-nitrosourea, benzo[a]pyrene, reproductive toxicity, oxidative stress inflammation

Introduction

Environmental exposure to toxic chemicals and their effects on the reproductive system have recently gained attention due to increases in chemical-induced reproductive dysfunction and in predisposing exposed individuals to infertility.[1] Studies have shown that oxidative stress (OS) plays a role in infertility pathophysiology,[2] with increasing evidence associating OS in

endometriosis, tubal, and peritoneal factor in infertility.[3] Reactive oxygen species (ROS) play various roles in the pathogenesis of the female reproductive tract.[4] OS can affect a variety of physiological functions in the reproductive tract, and excessive levels can result in precipitous pathologies affecting female reproduction.[5] ROS exerts its pathological effects via lipid damage, DNA fragmentation, ATP depletion, and inhibition of protein synthesis.[4] These may further affect a variety of physiological processes such as delayed oocyte maturation, ovarian steroidogenesis, ovulation, implantation, the formation of a blastocyst, luteolysis, and luteal maintenance in pregnancy.[6] N-methyl-N-nitrosourea (NMU) and BaP are chemical carcinogens that are commonly used to induce mammary tumors in female rats.[7–9] The specificity of NMU for mammary glands has been reported, and a single dose of NMU can give a 100% prevalence of tumor development.[10] Studies have reported increased generation of free radicals upon administration of NMU and BaP to female Wistar rats.[11] However, there is a lack of information on the combined effects of NMU and BaP on female rats' reproductive organs.

The use of plant-derived products in Africa to maintain human health has been common practice for a long time, and most people rely exclusively on herbal remedies[12] for their wellbeing. This practice is highly unregulated; the associated toxic effects of unstandardized herbal preparation cannot be emphasized, hence the need for careful monitoring. *C. portoricensis* (CP) is a permanent shrub[13] with evergreen small bipinnate leaves. Phytochemical analyses of *CP* revealed the presence of saponins, steroids, tannins, glycosides, alkaloids, and anthraquinones, among other compounds.[13] Leaves and roots of *CP* are used for preparing herbal remedies,[14,15] and they are also commonly used as a diuretic, worm emitter, as well as an abortifacient in Nigerian ethnopharmacology. *CP* has been experimentally validated to exhibit anticonvulsant, antidiarrheal, antispasmodic, antipyretic, antirheumatic, and analgesic effects in humans[13,16] and *in vitro* and *in vivo* antimicrobial activity.[15,17] Complementarily, *CP* displayed anticholinergic, antacid, antiulcer, molluscicidal, and ovicidal activities in experimental animals.[13]

Furthermore, *CP* has been shown to exhibit antioxidant, antiangiogenic,[18,19] and antiproliferative and pro-apoptotic effects *in vitro* in prostate cancer cells.[20] However, the protective effect of *CP* on female reproductive organs has not been documented. This study investigates the possible protective roles of *CP* against NMU- and BAP-induced reproductive damage in rats.

Materials and methods

Plant materials

Freshly harvested roots of *CP* (5.8 kg) were gathered from Agbogi Odofin Village (July 2016) in Osogbo (Nigeria). *CP* samples were verified and attested by experts from the Forest Research Institute of Nigeria (FHI number 111949). The root was air-dried and ground into a powdery form, which was soaked in *n*-hexane for defatting, and then separated with methanol (absolute) by the cold method of extraction. The methanol extract was further fractionated to obtain the chloroform fraction. This fraction was concentrated with a rotary evaporator to dryness at 40°C, with a yield of 0.74%.

Chemicals

NMU and BaP, 1-chloro-2,4-dinitrobenzene (CDNB), thiobarbituric acid (TBA), hydrogen peroxide (H_2O_2), epinephrine, glutathione (GSH) and 5′,5′-dithiobis-2-nitrobenzoic acid (DTNB) were procured from Sigma Chemical Company, (St. Louis, MO). NMU and BaP were dissolved in normal saline and kept in the dark at 4°C. Other reagents were of analytical grade, and were purchased from the British Drug Houses (Poole, Dorset, UK), and were of the purest quality available.

Animals

Five-week-old virgin female Sprague-Dawley rats (30–40 g), purchased from the Experimental Animal House, Faculty of Veterinary Medicine, Ibadan, Nigeria, were used for these experiments. The female rats were housed in rodent cages and kept in a well-ventilated experimental animal house. The ambient environment was maintained at a temperature and relative humidity of 25 ± 3°C, and 60 ± 10% respectively and a photoperiod of:12–12 h dark and light schedule. The rats were provided with standard rat pellets (Ladokun™ Feeds, Ibadan, Nigeria), access to clean drinking water *ad libitum*. They were acclimatized for two weeks before the commencement of the experiment. Experimental animals were sufficiently cared for as detailed in the "Guide for the Care and Use of Laboratory Animals" published by the National Institute of Health. Additionally, experimental protocols were approved by the Animal Welfare and Ethical Use of Laboratory Animal Committee University of Ibadan (UI-ACUREC/App/2015/061).

Experimental outline

Fifty-six rats weighing 30–40 g were randomly grouped into seven treatment groups of eight rats each and were treated for 10 consecutive weeks as follows:

Group 1: Control: received normal saline.
Group 2: NMU + BaP (50 mg/kg each)
Group 3: NMU + BaP and *CP* (50 mg/kg)
Group 4: NMU + BaP and *CP* (100 mg/kg)
Group 5: *CP* (100 mg/kg) only
Group 6: NMU + BaP and vincristine (0.5 mg/kg)
Group 7: Vincristine (0.5 mg/kg) only.
Rats were injected with NMU and BaP (50 mg/kg each) intraperitoneally at ages 7, 10, and 13 weeks old. The doses used for the i.p. injections for this study were based on previously published treatments in the literature.[21–23] *CP* was given orally thrice weekly, as previously described

from published work from our laboratory,[24] while vincristine (VIN) was administered intraperitoneally twice weekly. At the end of the 10th week, records of experimental rat's final body weights were taken, before blood collection via retro-orbital venous puncture into plastic sample tubes (without heparin coat). Subsequently, rats were sacrificed by cervical dislocation. Some uterus and ovary were harvested, weighed, recorded, and stored in 10% phosphate-buffered formalin for histopathology and immunohistochemistry (IHC) analyses. The remaining organs per group were homogenized separately in phosphate buffer (50 mmol/L & pH 6.8). The resulting mixture was spun in a centrifuge (at 10,000 g; 15 min). The resulting post-mitochondrial fraction was stored. Additionally, clotted blood was spun (3000 g; 15 min), and the serum obtained was stored at $-20°C$ until needed for further biochemical analyses.

Biochemical assays

Protein determination. Determination of serum protein levels was performed following Lowry's method, using bovine serum albumin (BSA) as a standard.[25] Briefly, Lowry reagent (0.7 mL) was added to the diluted sample or BSA standard (0.5 mL) and incubated (20 min at room temperature). Subsequently, diluted Folin's reagent (0.1 mL) was added to the reaction mixture, then mixed by rapid vortexing and incubated for another 30 min. Afterwards, the absorbance (at 750 nm) was acquired using a SpectraMax™ M3 Plate Reader (Molecular Devices, San Jose, CA). Values of protein were determined from the BSA generated calibration curve by simple extrapolation.

Determination of superoxide dismutase (SOD) activity

Following the method described by McCord and Fridovich,[26] the activity of SOD was determined. The process is based on the inhibition of autoxidation of epinephrine (pH 10.2) at 30°C. The assay mixture, containing sample (50 µL) and carbonate buffer (2.5 mL: 0.05 M; pH 10.2), was incubated and allowed to equilibrate, and then recently prepared adrenaline (0.3 mmol/L) of which 0.3 mL was added to the equilibrated reaction mixture and mixed gently by inverting the tube. With the aid of a spectrophotometer, absorbance (480 nm) was monitored at 30 s intervals for 150 s and the increase was recorded. SOD specific activity was calculated and expressed in Units/mg protein.

Determination of catalase activity

Using the method of Aebi,[27] catalase activity was determined from the samples. The reaction mixture, which was allowed to run for 3 min at 30 s intervals, comprises (50 µL of the sample, 2.4 mL of 50 mmol/L phosphate buffer (pH 7.0), and 1.0 mL of 19 mmol/L H_2O_2). Subsequently, the reaction was terminated by adding dichromate/acetic acid solution (2.0 mL) and heated for 10 min in a water bath (100°C). After that, the reacted solution was cooled at room temperature, and decreases in absorbance (at 570 nm) were recorded using a spectrophotometer. The specific activity of catalase was expressed as Units/mg protein.

Determination of glutathione-S-transferase (GST) activity

The activity of GST was determined as previously described by Habig *et al.*[28] using CDNB as a substrate. A volume of 1.7 mL phosphate buffer (100 mmol/L; pH 6.5) was added to 0.1 mL CDNB (30 mmol/L) to constitute a reaction mixture that was incubated for 5 min at 37°C. After that, the reaction was initiated with the addition of test samples (50 µL), and absorbance (340 nm) was monitored for 5 min, with records being taken. Additionally, a similarly constituted reaction mixture without the samples containing enzyme served as a reference blank. GST specific activity was conveyed as GSH/CDNB conjugate formed (µmoles)/min/mg protein referencing a standard extinction coefficient of 9.61/mmol/cm.

Assessment of the activities of glutathione peroxidase (GPx)

Utilizing the method of Rotruck *et al.*,[29] we determined the activities of GPx in samples from experimental rats. Sodium phosphate buffer (500 µL), 10.0 mmol/L sodium azide (100 µL), 4.0 mmol/L reduced GSH (200 µL), 2.5 mmol/L H_2O_2 (100 µL), and sample (50 µL) were reconstituted to form the reacting mixture. The reaction mixture was further made up to 2.0 mL with the addition of distilled water (1050 µL) and incubated (at 37°C, for 3 min). Subsequently, the reaction was stopped by adding 10% trichloroacetic acid (TCA; 500 µL) and centrifuged. The residual GSH was determined from the supernatant obtained after centrifugation, by adding 0.3 M disodium hydrogen phosphate (4.0 mL), and DTNB (1.0 mL). Finally, the absorbance at 412 nm was measured spectrophotometrically, and the obtained values of GPx activity were expressed in µmoles per mg protein.

Determination of reduced glutathione

GSH levels were determined according to the method of Moron *et al.*[16] Briefly, aliquots of uterine/ovarian homogenate were deproteinized by adding an equal volume of 4% sulfosalicylic acid and specific tissue homogenates. The mixture was subsequently subjected to cold centrifugation (4°C; 10,000 g; for 15 min). Following this, the resulting supernatant (100 µL) was added to DTNB (1.5 mL) and the absorbance at 412 nm was obtained by spectrophotometric reading. The GSH level was proportional to absorbance at 412 nm, and the values expressed in µmoles/g tissue.

Determination of the activities of myeloperoxidase (MPO)

The determination of MPO activity was achieved following the protocol described by Trush *et al.*,[30] using the reaction

between O-dianisidine and H_2O_2 and absorbance measured spectrophotometrically. MPO catalyzes the oxidation of O-dianisidine, with H_2O_2 serving as an oxidizing agent, to give a brown-colored oxidized O-dianisidine product, with characteristic absorbance at 460 nm. Aliquot of O-dianisidine (200 µL) and diluted H_2O_2 (50 µL) were added to the sample (7.0 µL). A unit of enzyme activity is defined as MPO that produced an absorbance change for 3 min at 460 nm.

Assessment of nitrate (nitric oxide) level

The amount of nitrite in supernatants or serum was assessed according to the methods of Palmer *et al.*[31] following the Griess reaction. Briefly, samples (0.5 mL) were mixed with Griess reagent (0.5 mL)—containing 1% sulfanilamide in 5% phosphoric acid and 0.1% *N*-(1-naphthyl) ethylenediamine dihydrochloride—and incubated at room temperature for 20 min. After that, spectrophotometric measures of the product absorbance (550 nm) were taken. With a standard solution as a reference point, total nitrite concentration was estimated by comparison with the absorbance.

Assessment of total sulfhydryl (TSH)

Following the method of Ellman,[32] the total thiol (TSH) level was evaluated. This method is predicated on the development of reasonably solid color (yellow) when Ellman's reagent—5,5'-dithiobis-2-nitro-benzoic acid—is reacted with compounds containing sulfhydryl groups. The chromophore produced from Ellman's reaction with reduced sulfhydryl groups possesses a molar absorption at 412 nm.

Determination of lipid peroxidation (LPO)

In brief, the sample (0.4 mL) was mixed with Tris-KCl buffer (1.6 mL)—containing 30% TCA (0.5 mL) to estimate LPO according to the method of Buege and Aust.[33] Subsequently, 0.75% TBA (0.5 mL) was added to each sample suspended in a hot water bath (80°C) and maintained at this temperature for 45 min. The reaction was then cooled in ice, followed by centrifugation at 3000 g. The absorbance of the resultant supernatant was obtained spectrophotometrically at 532 nm against a reference blank.

Histology

Isolated ovarian and uterine tissue samples were fixed in formalin (10%), dehydrated in ethanol (95%), and cleared with xylene before being embedded in paraffin. Subsequently, sections of about 3–4 µm of the tissue were prepared using a microtome from the paraffin-embedded gland and stained with hematoxylin and eosin (H&E).[34] Randomly, the tissue histology was observed under a light microscope, and histopathological abnormalities were scored by a pathologist who was blinded to the experimental treatment groups.

Immunohistochemistry

The kits for immunochemical staining were obtained from Abcam Chemical Inc. (Cambridge, MA), Santa Cruz Biotechnology (TX), and Dako Produktionsvej (Glostrup, Denmark). IHC of tissue sections from formalin-fixed ovary and uterus was employed to measure the protein expressions. The modified method of Chakravarthi *et al.*[35] was used for the immunohistochemical probing of tissues. The principle is based on the binding of a primary antibody (dilution of 1:100 or as given by the manufacturer) to a specific antigen. The antibody–antigen complex formed is incubated with a secondary, enzyme-conjugated antibody. In the presence of substrate and chromogen, the enzyme acts on the substrate to generate colored deposits at the sites of antibody-antigen binding, which was observed under a binocular microscope.[36] Cells with specific distinct color in the cytoplasm, cell membrane, or nuclei, depending on the antigenic sites were considered positive and compared with the controls. Method: tissue slides were deparaffinized (xylene 2x; 5 min each) and rehydrated sequentially in varying concentrations of ethanol (EtOH) twice for 3 min each (EtOH: 100%, 95%, and 70%). The slides were subsequently rinsed with wash buffer for 5 min each twice, followed by antigen retrieval using citrate (10 mM pH 6.0), and EDTA (pH 9.0) buffers. The slides were then preheated in a 24-slide Copling staining jar containing the buffer (250–300 mL) and incubated for 5 min (95–100°C). The slides were arranged in a staining hanger, dipped in the preheated buffer and, incubated for 10–20 min in a water bath. The staining container was removed to room temperature, and the slides were allowed to cool (for 20 min) in the retrieval buffer and rinsed (5 min, twice) with wash buffer. Blocking buffer (containing 10% BSA in PBS) was added to the slides and before incubation in a humidified chamber at room temperature for 15 min and then rinsed with wash buffer. Subsequently, the primed tissue slides were probed with diluted primary antibody (130 µL) and incubated in a humidified chamber at room temperature for 1 h. The slides were rinsed with wash buffer (5 min, twice) and, 130 µL of diluted biotinylated + streptavidin HRP secondary or polymeric-HRP anti-mouse/anti-rabbit was added, as appropriate, to the sections on the slides, and incubated for the specified time (polymer-single layer-30 min, LSAB-2 layers 15 min each). After that, the slides were washed with wash buffer (5 min, twice), and 130 µL diluted Sav-HRP conjugates were added to the slide sections, incubated for 15 min. After washing 130 µL of freshly prepared DAB substrate solution was added to the sections for color development until the desired color intensity was reached. The slides were repeatedly washed (thrice; 2 min) under running water. Slides were counterstained by immersion in hematoxylin for 10–20 s and rinsed under running tap water for 10 min, and dehydrated in EtOH: 95%; 95%; 100% and 100%, for 5 min intervals. The tissue slides were cleared in xylene thrice and mounted with a coverslip using a mounting solution. The color of the antibody staining in the tissue sections was observed under microscopy and then photographed.

Statistical analysis

Results were expressed as mean ± standard deviation (SD). Data were analyzed by one-way analysis of variance using SPSS version 23.0 (SPSS Inc., Chicago, IL). The differences were considered significant at P values <0.05.

Results

Effect of CP on body, uterine, and ovary weight of rats treated with NMU, BaP, and VIN

CP's effect on body and organ weight and relative organ weight of treated rats are shown in Table 1. Administration of NMU and BaP significantly ($P < 0.05$) decreased the rat weight gain relative to control by 32%, while *CP* (50 mg/kg and 100 mg/kg) treatment increased weight gain by 48% and 20%, respectively, relative to (NMU + BaP)-treated rats (Table 1). Furthermore, co-administration of NMU and BaP significantly increased the ovarian and uterine weight by 100% and 43%, respectively, when compared to the control. Also, the organo-somatic weight of the uterine and ovarian tissues in (NMU + BaP) rats significantly increased by 2.3 and 1.4 folds, respectively, when compared to the control. However, co-treatment with *CP* specifically at 100 mg/kg decreased ($P < 0.05$) the ovarian and uterine weight by 50% and 33%, as well as organo-somatic weight by 57% and 38%, respectively, when compared to the control and standard (VIN; Table 1).

Effect of CP on uterine and ovary antioxidant status of rats treated with NMU, BaP, and VIN

Malondialdehyde (MDA; index of OS) increased markedly in the ovarian tissue of (NMU + BaP)-treated rats by 58% compared to the control. Following *CP* (50 and 100 mg/kg) co-treatment, the marked increase in ovarian MDA was reduced ($P < 0.05$) by 29% and 44%, respectively (Table 2). Also, ovarian and uterine GPx and TSH markedly decreased in (NMU + BaP) administered rats relative to the control. To be specific, *CP* (50 and 100 mg/kg) co-treatment restored ovarian and uterine GPx and TSH to values that were statistically similar to the control (Tables 2 and 3). Furthermore, there were decreases ($P < 0.05$) in the activities of uterine and ovarian GST, and uterine catalase in (NMU + BaP) administered rats relative to controls. *CP* (50 and 100 mg/kg) treatment decreased the activities of uterine and ovarian GST and catalase in (NMU + BaP) rats (Figure 1). There were no differences ($P > 0.05$) in uterine and ovarian GSH levels in (NMU + BaP) rats relative to others (Tables 2 and 3).

Table 1. Effect of *CP* extracts on body and organ weight of rats treated with *N*-methyl-*N*-nitrosourea (NMU) and benzo[a]pyrene (BaP).

| | Body weight (g) | | | Uterus | | Ovary | |
	Initial	Final	Weight gain	Weight (g)	OSIa (g)	Weight (g)	OSI[a] (g)
Control	51.32 ± 2.87	144.97 ± 4.48	95.73 ± 1.45	0.11 ± 0.01	0.07 ± 0.03	0.07 ± 0.02	0.05 ± 0.02
NMU + BAP	63.83 ± 1.51	141.13 ± 6.00	65.33 ± 6.54*	0.22 ± 0.03*	0.16 ± 0.08*	0.10 ± 0.02*	0.07 ± 0.02*
NMU + BAP + CP1	68.89 ± 2.68	167.00 ± 2.34	96.50 ± 2.76**	0.23 ± 0.03**	0.14 ± 0.06*	0.09 ± 0.02*	0.05 ± 0.03
NMU + BAP + CP2	73.09 ± 4.25	151.08 ± 4.48	78.94 ± 5.63	0.15 ± 0.02**	0.10 ± 0.03	0.05 ± 0.01	0.03 ± 0.02
CP2 only	54.84 ± 2.01	136.38 ± 3.94	85.76 ± 2.71	0.18 ± 0.01	0.13 ± 0.06	0.08 ± 0.02	0.06 ± 0.01
NMU + BAP + VIN	80.44 ± 5.56	165.8 ± 4.59	86.47 ± 8.82	0.08 ± 0.01	0.05 ± 0.02	0.06 ± 0.00	0.04 ± 0.01
VIN only	66.02 ± 2.47	141.25 ± 8.80	64.47 ± 3.97	0.15 ± 0.04	0.11 ± 0.03	0.08 ± 0.00	0.06 ± 0.01

NMU: *N*-methyl-*N*-nitrosourea; *CP*: *Calliandra portoricensis*; BaP: benzo[a]pyrene; VIN: vincristine; OSI: organo-somatic index; *CP*1 = 50 mg/kg; *CP*2 = 100 mg/kg;
a% of final weight.
Values are expressed as mean ± standard deviation of 8 animals per group.
*Significantly ($P < 0.05$) different from control.
**($P < 0.05$) different from (NMU + BaP).

Table 2. Effect of CP on uterine antioxidant parameters in rats treated with *N*-methyl-*N*-nitrosourea (NMU) and Benzo[a]pyrene (BaP).

Groups	LPO (μM/mg protein)	GSH (μg/mL/ mg protein)	GPx (U/mg protein)	Total sulfhydryl (μmol/L)
Control	6.97 ± 0.96	19.64 ± 0.35	182.5 ± 2.65	19.44 ± 0.79
NMU + BaP	7.17 ± 1.05	18.94 ± 0.31	101.8 ± 0.28*	11.76 ± 1.54
NMU+ BaP+ CP1	6.57 ± 1.08	18.71 ± 0.40	163.5 ± 10.88	15.70 ± 3.43*
NMU + BaP+ CP2	8.06 ± 0.92	18.76 ± 0.94	171.7 ± 8.58**	17.23 ± 3.48**
CP	5.41 ± 1.73	19.53 ± 0.87	203.0 ± 18.29	21.68 ± 2.11
NMU+ BaP+ VIN	6.24 ± 1.35	20.48 ± 0.71	100.5 ± 16.96	20.20 ± 4.61
VIN	6.09 ± 0.82	20.06 ± 0.48	111.2 ± 0.48	20.93 ± 2.30

NMU: *N*-methyl-*N*-nitrosourea; *CP*: *Calliandra portoricensis*; BaP: benzo[a]pyrene; VIN: vincristine; *CP*1 = 50 mg/kg; *CP*2 = 100 mg/kg.
Values are expressed as mean ± standard deviation of 8 animals per group.
*Significantly ($P < 0.05$) different from control.
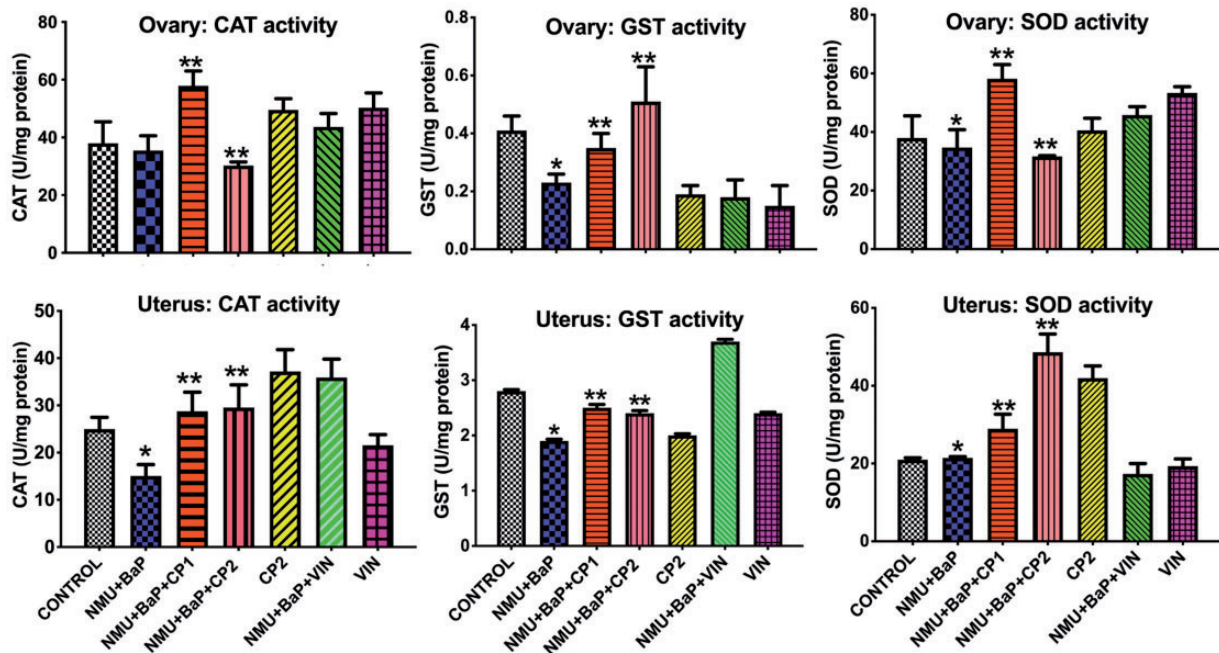**($P < 0.05$) different from (NMU + BaP).

Table 3. Effect of CP on ovarian antioxidant parameters in rats treated with *N*-methyl-*N*-nitrosourea (NMU) and benzo[a]pyrene (BaP).

Grouping	LPO (μM/mg protein)	GSH (μg/mL/ mg protein)	GPx (U/mg protein)	Total sulfhydryl (μmol/L)
Control	5.82 ± 1.51	24.40 ± 0.57	219.42 ± 46.28	0.26 ± 0.04
NMU + BaP	$9.22 \pm 1.74^*$	23.76 ± 0.68	$149.13 \pm 11.87^*$	$0.14 \pm 0.11^*$
NMU+ BaP+ *CP*1	$6.54 \pm 1.46^{**}$	23.50 ± 0.62	$184.74 \pm 19.91^{**}$	0.21 ± 0.45
NMU + BaP + *CP*2	$5.13 \pm 1.05^{**}$	23.16 ± 0.71	$185.49 \pm 2.64^{**}$	$0.23 \pm 0.02^{**}$
CP only	5.74 ± 0.73	25.68 ± 0.41	288.72 ± 22.93	0.28 ± 0.08
NMU + BaP + VIN	8.27 ± 1.88	23.88 ± 1.08	$252.29 \pm 24.49^{**}$	0.21 ± 0.09
VIN only	6.43 ± 0.83	24.74 ± 0.44	287.99 ± 28.93	0.28 ± 0.17

NMU: *N*-methyl-*N*-nitrosourea; *CP*: *Calliandra portoricensis*; BaP: benzo[a]pyrene; VIN: vincristine; *CP*1 = 50 mg/kg; *CP*2 = 100 mg/kg.
Values are expressed as mean ± standard deviation of 8 animals per group.
*Significantly ($P < 0.05$) different from control.
**($P < 0.05$) different from (NMU + BaP).

Figure 1. Ovarian and uterine CAT, GST and SOD activities in rats treated with NMU, BaP, *CP*, and VIN. Values are expressed as mean ± SD ($n = 8$), *significantly ($P < 0.05$) different from control, **different ($P < 0.05$) from NMU + BaP. ($P < 0.05$). CAT: catalase; GST: glutathione-*S*-transferase; SOD: superoxide dismutase; NMU: *N*-methyl-*N*-nitrosourea; BaP: benzo[a]pyrene; VIN: vincristine; *Calliandra portoricensis* (*CP*) *CP*1 = 50 mg/kg; *CP*2 = 100 mg/kg. (A color version of this figure is available in the online journal.)

Effect of CP on markers of inflammation in uterus and ovary of rats treated with NMU, BaP, and VIN

In rats (NMU + BaP), the activities of ovarian and uterine MPO increased ($P < 0.05$) by 409% and 38.9%, ovarian, and uterine nitric oxide levels by 107% and 18%, respectively, compared to the control (Figure 2). However, co-administration of *CP* significantly attenuated the ovarian and uterine MPO by 60% and 140%, respectively, relative to (NMU + BaP) rats. Similarly, *CP* at 50 and 100 mg/kg decreased ovarian NO relative to (NMU + BaP) rats.

Effect of CP on histology and protein expression in rats treated with NMU, BaP, and VIN

Figures 3 to 8 show histology of the uterus and ovary and the expression of proteins, namely: Bcl-2, caspase 3, inducible nitric oxide synthase (iNOS) (ovarian), BAX (ovarian),

and p53 (ovarian). Photomicrographs showed a typical architecture of uterus, with a healthy endometrium epithelial layer and endometrial gland in the control group, while the (NMU + BaP)-treated group had a severely infiltrated endometrial gland and inflamed stromal cells (Figure 3). Besides, the ovarian architecture appears normal in the control with healthy connective tissues and theca cells layer. At the same time, the (NMU + BaP) administered group showed ovarian stroma with fibrosis and vascular congestion along with degenerated cells (Figure 3). However, co-treatment with VIN and *CP* attenuated ($P < 0.05$) these observations. Furthermore, the administration of NMU and BaP caused a high expression of iNOS and Bcl-2 proteins in ovarian tissues when compared to the control (Figures 4 and 6). However, co-treatment with *CP* significantly reduced the expression of these proteins. Also, the (NMU + BaP) group had a milder expression of caspase-3,
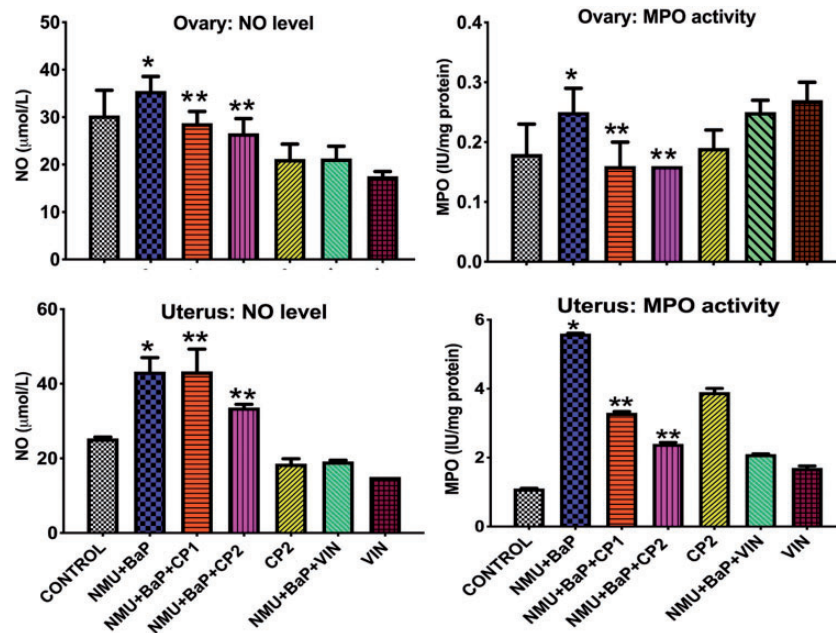
Figure 2. Ovarian and uterine NO levels and MPO activities in rats treated with NMU, BaP, *CP*, and VIN. Values are expressed as mean ± SD ($n = 8$), *significantly ($P < 0.05$) different from control, **different ($P < 0.05$) from NMU + BaP ($P < 0.05$). NO: nitric oxide; MPO: myeloperoxidase; NMU: *N*-methyl-*N*-nitrosourea; BaP: benzo[a]pyrene; VIN: vincristine; *Calliandra portoricensis* (*CP*) *CP*1 = 50 mg/kg; *CP*2 = 100 mg/kg. (A color version of this figure is available in the online journal.)
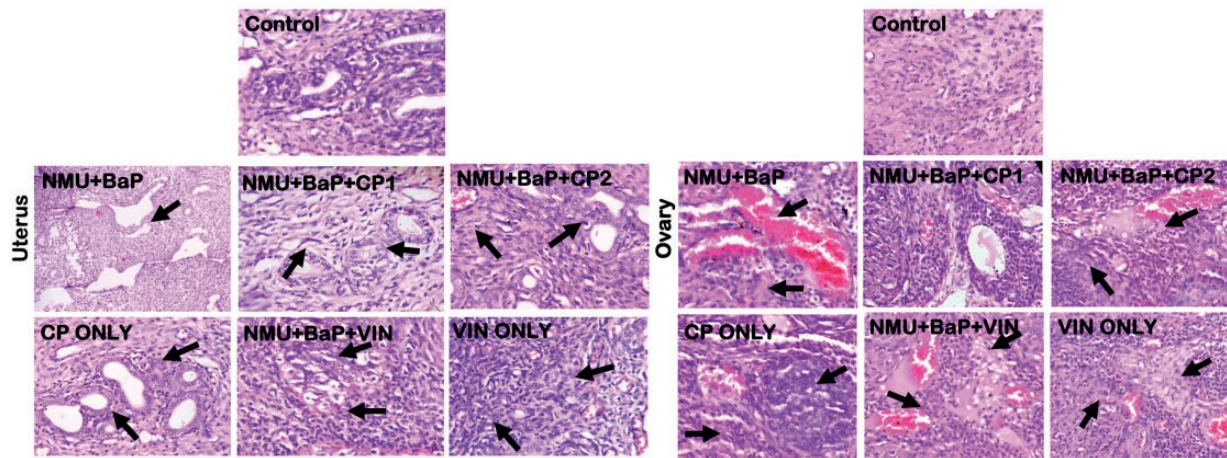
Figure 3. Photomicrograph of rat uterine and ovarian tissue showing the effect of *CP* co-treatment with NMU, BaP, and VIN. (a) Uterus (left panel): control shows normal myometrium, with few inflammatory cells in the endometrial stroma. NMU + BaP: exhibiting atypical endometrial cells with macronuclei. NMU + BaP + *CP*1: appears normal with moderate epithelial degeneration. NMU + BaP + *CP*2: epithelial cells are mildly thickened, with few inflammatory cells, but myometrium appears normal. *CP*2: endometrial epithelial and myometrium appears normal with moderate hyperplasia and dilation. NMU + BaP + VIN: epithelial appears moderately normal, endometrial gland appears normal. VIN: endometrium and endometrial glands appear normal, with moderate inflammatory cells in the stroma. The myometrium also appears normal (black arrow). (b) Ovary (right panel): control shows normal Graafian follicles with normal theca cells within the ovarian cortex (black arrow). NMU + BaP: exhibited some developmental follicle, including primordial and normal theca cells, degenerated lutein cells with ovarian stroma showing mild fibrosis (black arrow). NMU + BaP + *CP*1: show normal Graafian follicle with normal theca cells within the ovarian cortex, the ovarian cells appear normal with normal connective tissues. NMU + BaP + *CP*2: normal Graafian follicles with mild theca cell degeneration, ovarian stroma shows moderate vascular congestion, and the stroma connective tissues appear normal. *CP*2: few normal Graafian follicles and theca cells with few atretic follicles within the ovarian cortex. NMU + BaP + VIN: Graafian follicles, vessels, connective tissues, and theca cells appears normal. VIN: shows normal Graafian follicles with normal theca cells, luteinize cells exhibited moderate hyperplasia. NMU: *N*-methyl-*N*-nitrosourea; BaP: benzo[a]pyrene; VIN: vincristine; *Calliandra portoricensis* (*CP*) *CP*1 = 50 mg/kg; *CP*2 = 100 mg/kg. H&E stained, magnification 400×. (A color version of this figure is available in the online journal.)

Bax, and p53 in ovarian tissues relative to the control (Figures 5, 7, and 8), while co-treatment with *CP* as well as a standard drug (VIN) increased the expression of these proteins. However, in uterine tissue, treatment with NMU and BaP reduced caspase-3 relative to the control. The expression of caspase-3 was highly elevated following co-treatment with *CP* when compared to the control (Figure 5). Also, the expression of uterine Bcl-2 was sharply increased in the (NMU + BaP) group relative to the control (Figure 4). Co-treatment with *CP* reduced the expression of Bcl-2 when compared to the control.
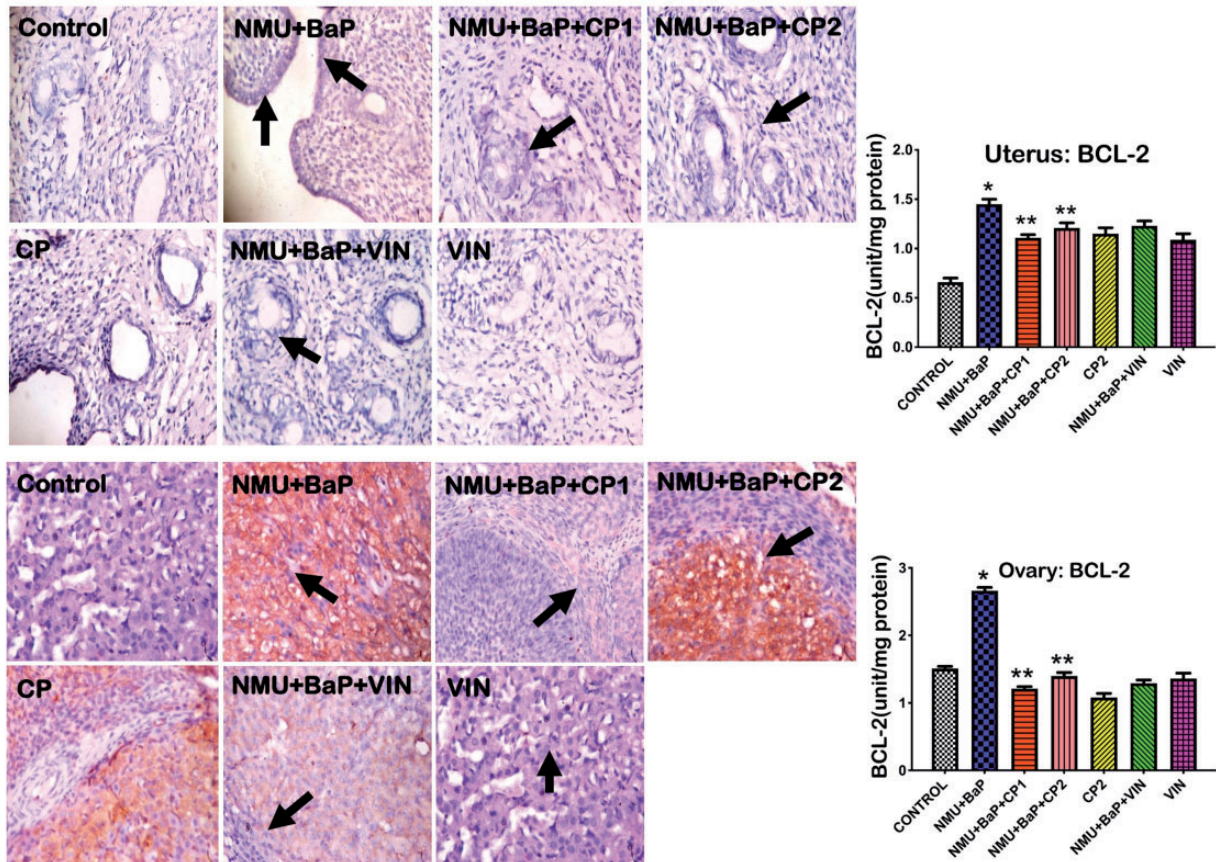
Figure 4. Immunohistochemistry staining showing the effect of *CP*, NMU, and BaP co-treatment on uterine (top panel) and ovarian (lower panel) Bcl-2 expression. Values are expressed as mean $\pm$ SD ($n = 8$), *significantly ($P < 0.05$) different from control, **different ($P < 0.05$) from NMU + BaP. ($P < 0.05$). *CP*: *Calliandra portoricensis*; NMU: *N*-methyl-*N*-nitrosourea; BaP: benzo[a]pyrene; VIN: vincristine; *CP*1 = 50 mg/kg; *CP*2 = 100 mg/kg, magnification 400×. (A color version of this figure is available in the online journal.)

Effect of CP on reproductive hormones in (NMU + BaP) rats

The hormonal status of uterine and ovarian tissues is presented in Figures 9 to 12. Administration of NMU and BaP caused a significant decrease in follicle stimulating hormone (FSH) and prolactin levels in uterine tissues relative to the control. In contrast, progesterone was upregulated in the (NMU + BaP)-induced group when compared to the control group. Following co-treatment with *CP*, the reduction in FSH and prolactin hormone levels were improved in the rats. Progesterone expression was also reduced following co-treatment with *CP*. Besides, (NMU + BaP) rats showed a lower expression of ovarian FSH and LH hormones. In contrast, a higher expression of progesterone was observed compared to the control. *CP* co-treatment appreciably upregulated FSH, LH, and downregulated progesterone in the rats.

Discussion

Nature has been the primary source of medical healing from ancient times. Even today, plant-based medicine plays a vital role in the primary health care of approximately 80% of the world's population, mainly in Africa.[12] Our current findings show that the chloroform fraction of *CP* attenuates NMU and BaP-induced OS and inflammatory

reactions in the uterine and ovarian tissues of experimental animals.

The relationship of NMU toxicity to OS is firmly established.[7] Overproduction of ROS and a decline in the antioxidant defense mechanisms may shift the oxidant versus antioxidant equilibrium.[6] Importantly, the cell requires a definite quantity of ROS for the proper running of cell functions, presuming that every molecule is reversed to their reduced state upon oxidation.[37] In this study, NMU + BaP-induced toxicity was evident by a marked increase in MDA and NO levels. The toxicity was accompanied by a significant downturn in enzymatic defense activities of SOD, CAT, TSH, and GSH in uterine and ovarian tissues. Leukocytes primarily express the enzyme MPO, and it is frequently released when activation and degranulation of leukocytes occur. MPO can generate oxidants and free radicals that inadvertently promote LPO and infiltration of inflammatory sites by neutrophils.[38,39]

Additionally, the formation of nitric oxide from L-arginine catalyzed by the enzyme nitric oxide synthase (NOS) may play a vital role in immune system modulation, vascular tone, and neurotransmission.[40] Regions of ovarian and uterine inflammation are established foci of free radicals' generation, e.g., NO and several species of oxygen radicals. In this study, increased MPO activity and NO level were observed, suggesting the onset of chronic
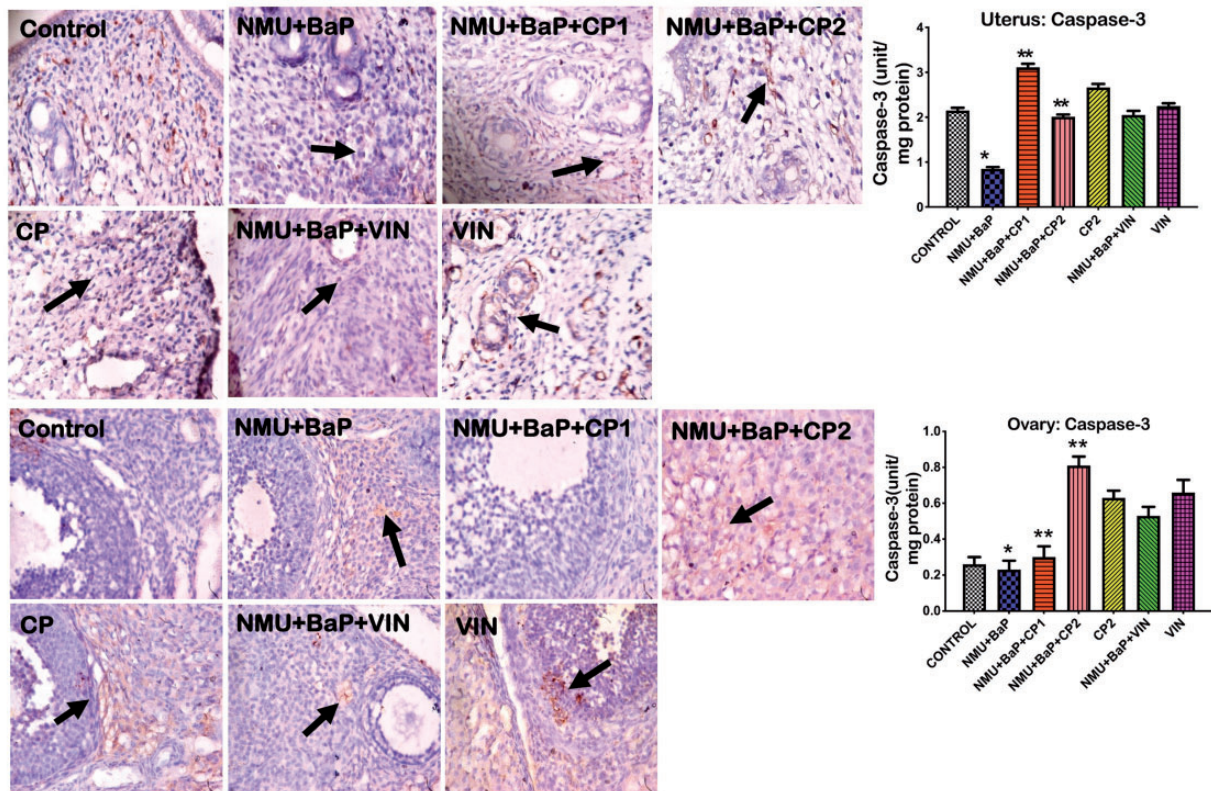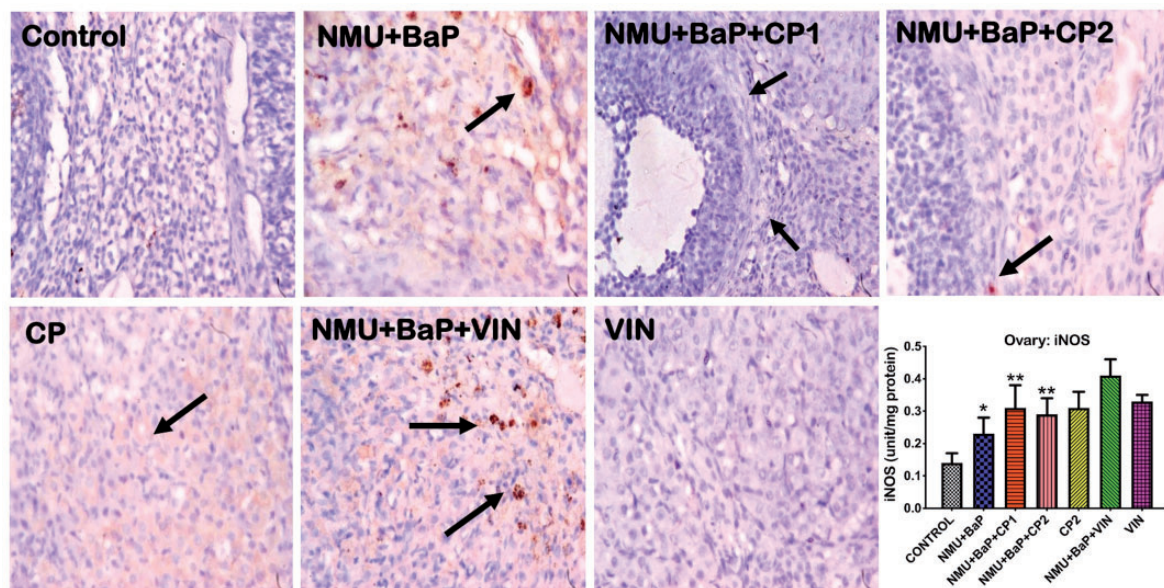
Figure 5. Immunohistochemistry staining showing the effect of *CP*, NMU, and BaP co-treatment on uterine (top panel) and ovarian (lower panel) caspase-3 expression. Values are expressed as mean ± SD ($n = 8$), *significantly ($P < 0.05$) different from control, **different ($P < 0.05$) from NMU + BaP ($P < 0.05$). *CP*: *Calliandra portoricensis*; NMU: *N*-methyl-*N*-nitrosourea; BaP: benzo[a]pyrene; VIN: vincristine; *CP*1 = 50 mg/kg; *CP*2 = 100 mg/kg, magnification 400×. (A color version of this figure is available in the online journal.)

Figure 6. Immunohistochemistry staining showing the effect of *CP*, NMU, and BaP co-treatment on ovarian on iNOS expression. Values are expressed as mean ± SD ($n = 8$), *significantly ($P < 0.05$) different from control, **different ($P < 0.05$) from NMU + BaP ($P < 0.05$). *CP*: *Calliandra portoricensis*; NMU: *N*-methyl-*N*-nitrosourea; BaP: benzo[a]pyrene; VIN: vincristine; *CP*1 = 50 mg/kg; *CP*2 = 100 mg/kg, magnification 400×. (A color version of this figure is available in the online journal.)

inflammation in rat uterus and ovaries. This observation is in line with reports by previous authors.[41,42] In the light of these findings, rat ovarian and uterine LPO may have resulted from increased production of highly reactive ROS, that reacts with polyunsaturated fatty acids present in phospholipid constituents of cell membranes, naturally present in uterine and ovarian tissues of experimental rats, that may consequently lead to organ dysfunction.[24,41]
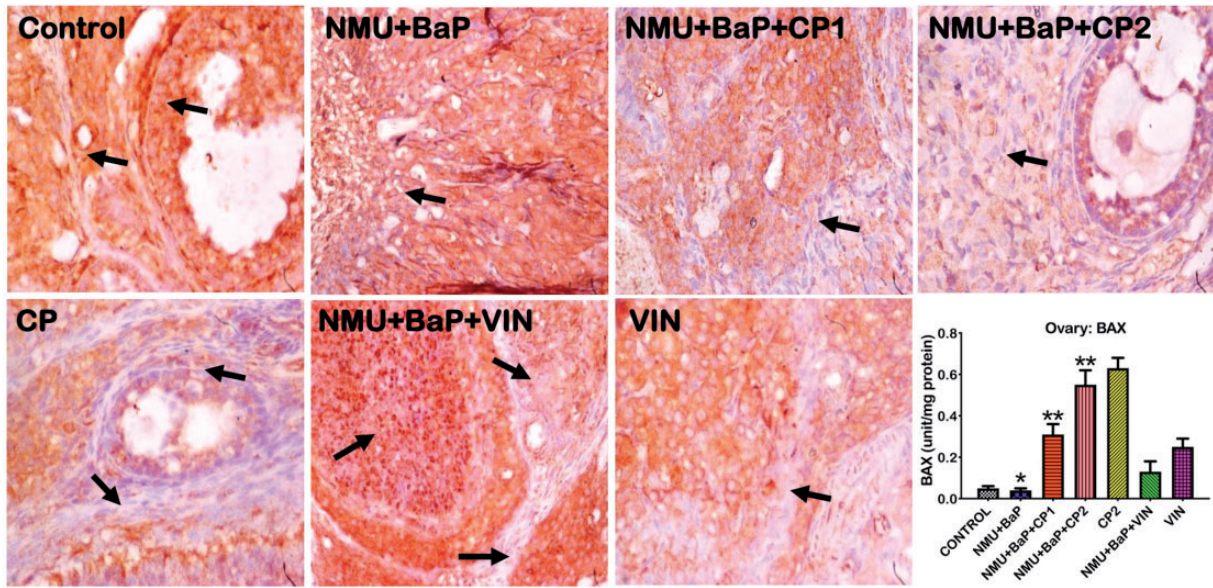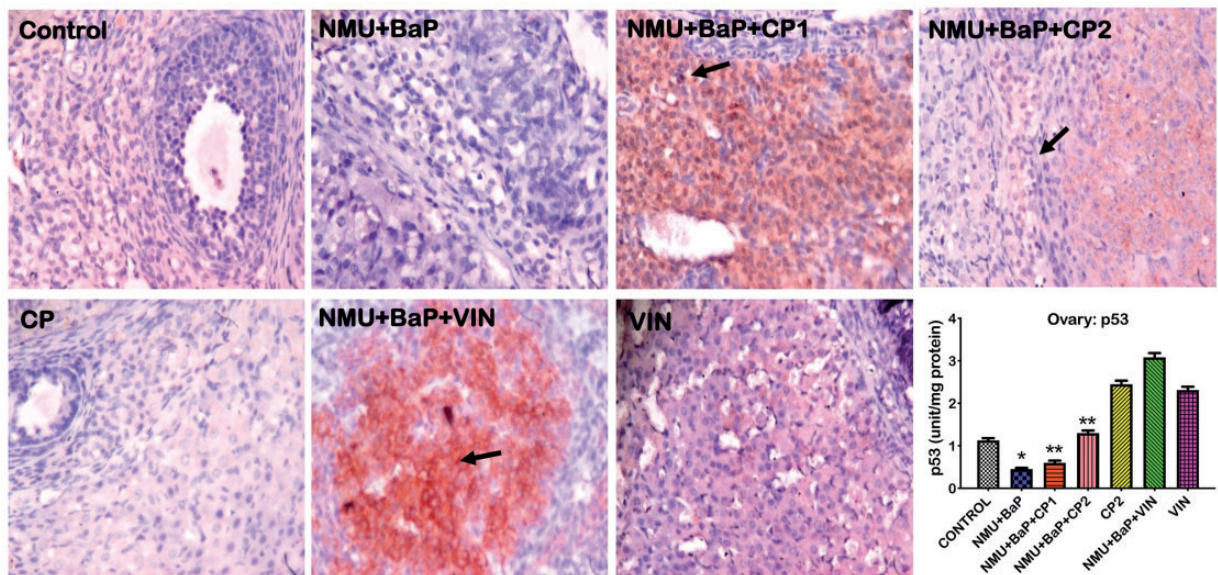
Figure 7. Immunohistochemistry staining showing the effect of *CP*, NMU, and BaP co-treatment on ovarian Bax expression. Values are expressed as mean ± SD ($n = 8$), *significantly ($P < 0.05$) different from control, **different ($P < 0.05$) from NMU + BaP ($P < 0.05$). CP: *Calliandra portoricensis*; NMU: *N*-methyl-*N*-nitrosourea; BaP: benzo[a]pyrene; VIN: vincristine; $CP1 = 50$ mg/kg; $CP2 = 100$ mg/kg, magnification 400×. (A color version of this figure is available in the online journal.)

Figure 8. Immunohistochemistry staining showing the effect of *CP*, NMU, and BaP co-treatment on ovarian *p53* expression. Values are expressed as mean ± SD ($n = 8$), *significantly ($P < 0.05$) different from control, **different ($P < 0.05$) from NMU + BaP ($P < 0.05$). CP: *Calliandra portoricensis*; NMU: *N*-methyl-*N*-nitrosourea; BaP: benzo[a]pyrene; VIN: vincristine; $CP1 = 50$ mg/kg; $CP2 = 100$ mg/kg, magnification 400×. (A color version of this figure is available in the online journal.)

Increases in MDA level, as well as a decrease in antioxidative defense enzymes, further corroborate previous reports on NMU-induced mammary carcinogenesis.[24] The GST and GPx activities were also drastically decreased after (NMU + BaP) intoxication. However, treatment with *CP* markedly restored antioxidant status and decreased inflammatory indices in the rats, supporting the *in vitro* antioxidant effect of *CP* as previously reported.[18]

Apoptosis is a critical process that regulates cancer promotion and progression. Cancer cells avoid apoptosis and continue to proliferate without any control. p53 (wild-type) participates in programmed cell death when DNA damage

occurs in cells.[43,44] By default, signals that activate the p53 response result in a quick increase in protein TP53, via stabilization of the protein and DNA binding function activation.[45] TP53 functions as a transcription activator of other targets downstream, including p21 and Bax, signifying that p53 can activate different pathways, including apoptosis.[45–47] Previous studies have demonstrated *CP*'s ability to impede various types of human cancer cell growth via alteration of key apoptotic signaling pathways.[20,48]

Similarly, *CP*-induced apoptosis in cancer cells is mediated by mitochondrial function alterations and other critical qualities of apoptosis, such as caspase activation and
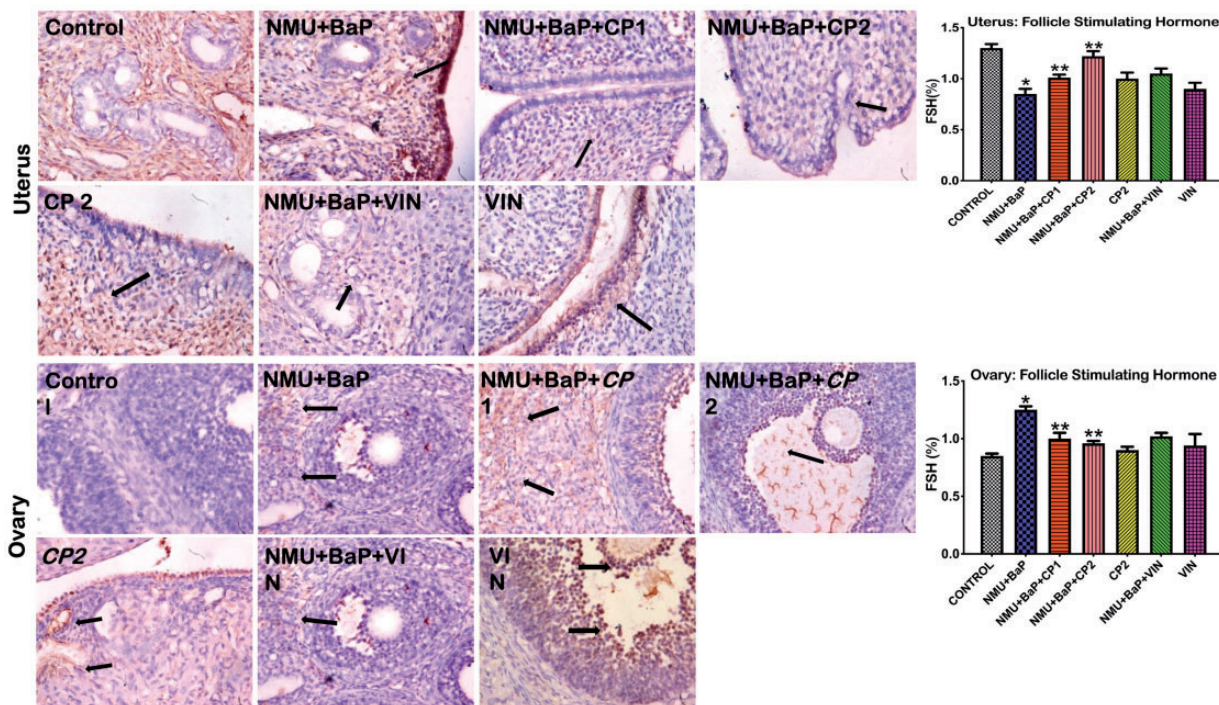
Figure 9. Immunohistochemistry staining showing the effect of *CP*, NMU, and BaP co-treatment on uterine (top panel) and ovarian (lower panel) FSH expression. Values are expressed as mean ± SD ($n = 8$), *significantly ($P < 0.05$) different from control, **different ($P < 0.05$) from NMU + BaP ($P < 0.05$). *CP*: *Calliandra portoricensis*; NMU: *N*-methyl-*N*-nitrosourea; BaP: benzo[a]pyrene, FSH: follicle stimulating hormone; VIN: vincristine; *CP*1 = 50 mg/kg; *CP*2 = 100 mg/kg, magnification: 400×. (A color version of this figure is available in the online journal.)
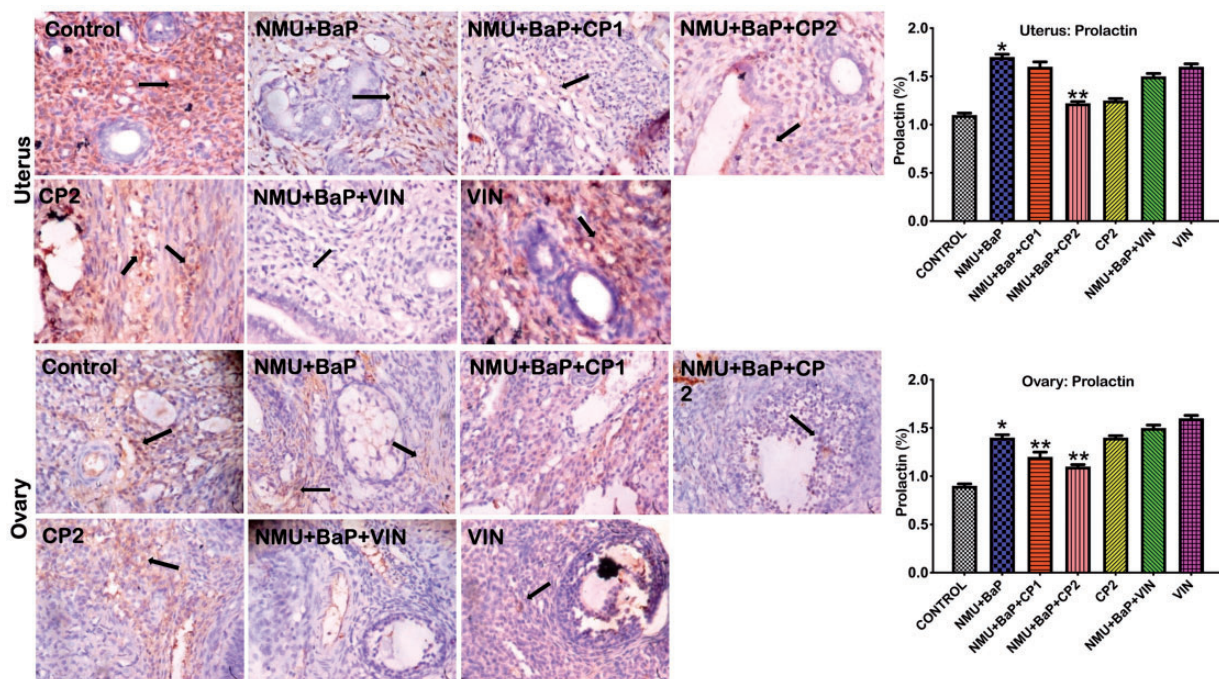

Figure 10. Immunohistochemistry staining showing the effect of *CP*, NMU, and BaP co-treatment on uterine (top panel) and ovarian (lower panel) prolactin expression. Values are expressed as mean ± SD ($n = 8$), *significantly ($P < 0.05$) different from control, **different ($P < 0.05$) from NMU + BaP. ($P < 0.05$). *CP*: *Calliandra portoricensis*; NMU: *N*-methyl-*N*-nitrosourea; BaP: benzo[a]pyrene; FSH: follicle stimulating hormone; VIN: vincristine; *CP*1 = 50 mg/kg; *CP*2 = 100 mg/kg, magnification: 400×. (A color version of this figure is available in the online journal.)

nuclear fragmentation,[37,38] according to previous reports. In this study, we tested the pro-apoptotic and anti-inflammatory effects of *CP* on the ovary and uterus. Our results demonstrated that the protein expression of uterine COX 2, iNOS, and BCL2 was higher in NMU + BaP rats relative to the control. This observation is in line with the study of Abolaji et al.,[49] who reported on 6-gingerol- from ginger phyto-protection against chlorpyrifos-induced
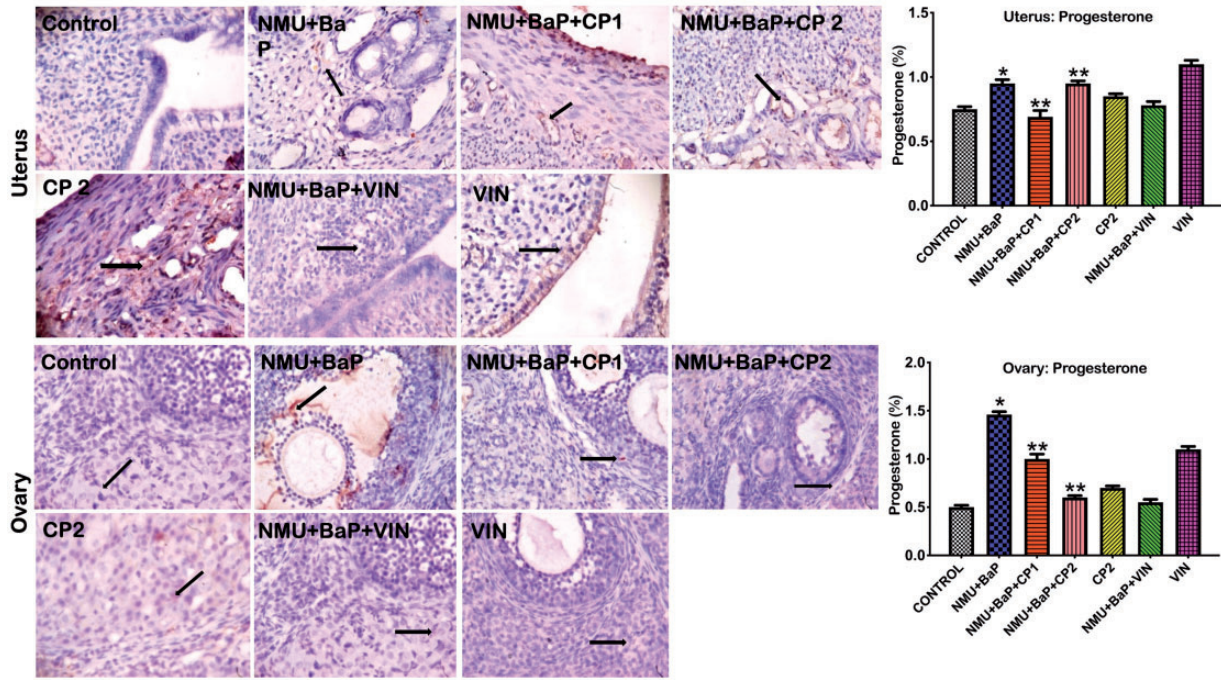
Figure 11. Immunohistochemistry staining showing the effect of *CP*, NMU, and BaP co-treatment on uterine (top panel) and ovarian (lower panel) progesterone expression. Values are expressed as mean ± SD ($n = 8$), *significantly ($P < 0.05$) different from control, **different ($P < 0.05$) from NMU + BaP. ($P < 0.05$). *CP*: *Calliandra portoricensis*; NMU: *N*-methyl-*N*-nitrosourea; BaP: benzo[a]pyrene; FSH: follicle stimulating hormone; VIN: vincristine; *CP*1 = 50 mg/kg; *CP*2 = 100 mg/kg, magnification: 400×. (A color version of this figure is available in the online journal.)
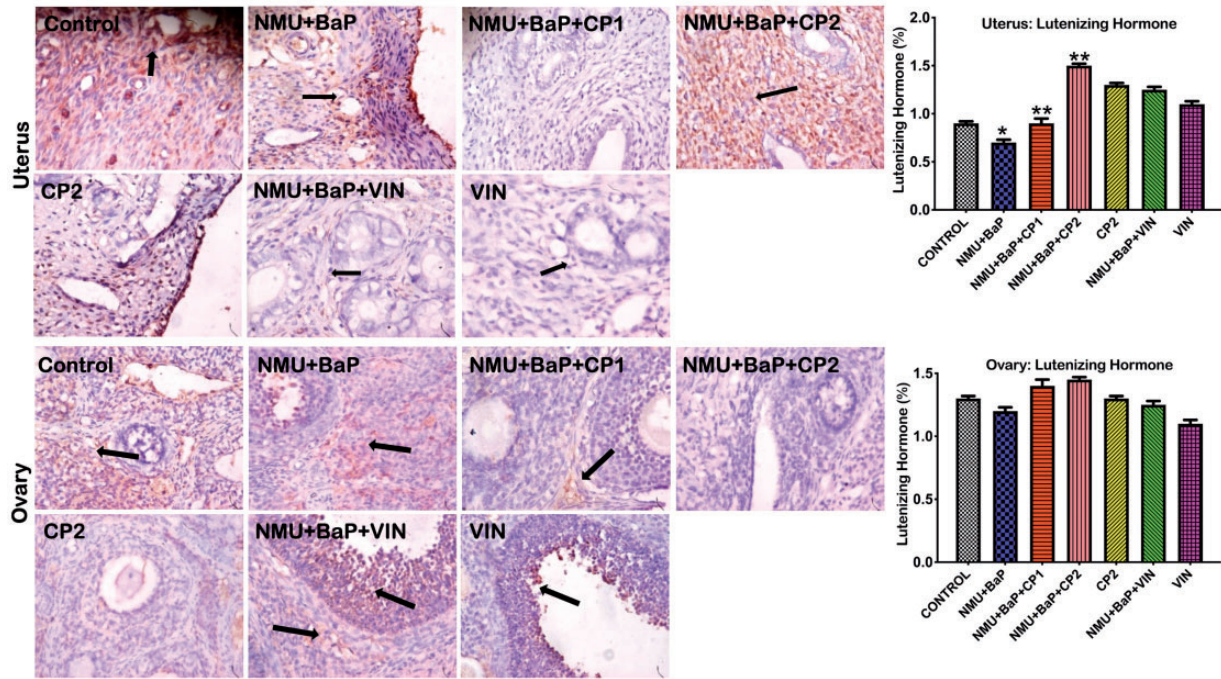

Figure 12. Immunohistochemistry staining showing the effect of *CP*, NMU, and BaP co-treatment on uterine (top panel) and ovarian (lower panel) luteinizing hormone expression. Values are expressed as mean ± SD ($n = 8$), *significantly ($P < 0.05$) different from control, **different ($P < 0.05$) from NMU + BaP ($P < 0.05$). *CP*: *Calliandra portoricensis*; NMU: *N*-methyl-*N*-nitrosourea; BaP: benzo[a]pyrene, FSH: follicle-stimulating hormone; VIN: vincristine; *CP*1 = 50 mg/kg; *CP*2 = 100 mg/kg, magnification: 400×. (A color version of this figure is available in the online journal.)

inflammatory damage in rats. Importantly, the chloroform fraction of *CP* at 100 mg/kg significantly improved cox-2, iNOS, and bcls in uterine and ovarian tissues, suggesting the pro-apoptotic and anti-inflammatory roles of *CP*.

Furthermore, the pro-apoptotic effect of *CP* was confirmed by the increased expression of proteins of Bax and caspase-3 in ovarian and uterine tissues. The present results conform to the previous report on the *CP*-induced increase

in Bax protein expression and caspase-3.[50] The p53 is a tumor suppressor gene, an efficient inhibitor of cell growth, promoter of cell cycle arrest, and apoptosis.[20,51] Therefore, the control of p53 is essential to allow both healthy cell growth and tumor suppression.[52] The ability of *CP* to upregulate the expression of p53 protein in uterine and ovarian tissues of (NMU + BaP) rats further supported its anticancer property.

Hormonal imbalance is one of the leading causes of female infertility since it may impair ovulation. Normal levels of LH, FSH, and progesterone are needed to stimulate the egg release, preparation of uterus, and implantation of the fertilized egg. In this study, rats treated with NMU + BaP had a mild expression of LH, FSH, and progesterone. This observation confirms the findings of Yuri *et al.*, who reported that "Human chorionic gonadotropin (hCG) inhibits NMU-mediated mammary carcinoma growth in female Lewis rats",[53] and Gehring *et al.* alluded to the controversial role of hCG in tumor development.[54] The ability of *CP* to attenuate the expression of these hormones points to its pro-fertility role in animals. The histology of the uterus and ovary from NMU + BaP rats revealed extensive architectural distortion and infiltration of inflammatory cells. These alterations were significantly decreased in NMU + BaP rats given *CP.* The histological findings further corroborated the biochemical data supporting the ameliorative potential of *CP* in NMU + BaP intoxicated rats.

In conclusion, NMU and BaP co-exposure resulted in ovarian and uterine toxicity in rats due to extensive inflammation and OS. Treatment with *CP* significantly ameliorated the toxicity through mechanisms that involve pro-apoptotic, anti-inflammatory, and antioxidant activities.

AUTHORS CONTRIBUTIONS

All authors participated in the design, interpretations of the study, data analysis, and review of the manuscript; OAA and SO conceptualized the experiments, AA and JM carried out a preliminary analysis of the data. AA and JM: carried out the research. OAA, SO, supervised the investigation. OAA, AA, and JM proof check data for error. AA, JM, OAA, and SO wrote and revised the manuscript.

DECLARATION OF CONFLICTING INTERESTS

The author(s) declared no potential conflicts of interest with respect to the research, authorship, and/or publication of this article.

FUNDING

ORCID IDS

Solomon E Owumi https://orcid.org/0000-0002-4973-0376
Oluwatosin A Adaramoye https://orcid.org/0000-0001-9960-6763

REFERENCES

1. Iorio R, Castellucci A, Ventriglia G, Teoli F, Cellini V, Macchiarelli G, Cecconi S. Ovarian toxicity: from environmental exposure to chemotherapy. *Curr Pharm Des* 2014;**20**:5388–97
2. Elmorsy E, Al-Ghafari A, Aggour AM, Mosad SM, Khan R, Amer S. Effect of antipsychotics on mitochondrial bioenergetics of rat ovarian theca cells. *Toxicol Lett* 2017;**272**:94–100
3. Antherieu S, Bachour-El Azzi P, Dumont J, Abdel-Razzak Z, Guguen-Guillouzo C, Fromenty B, Robin MA, Guillouzo A. Oxidative stress plays a major role in chlorpromazine-induced cholestasis in human HepaRG cells. *Hepatology* 2013;**57**:1518–29
4. Sen N, Liu X, Craig ZR. Short term exposure to di-n-butyl phthalate (DBP) disrupts ovarian function in young CD-1 mice. *Reprod Toxicol* 2015;**53**:15–22
5. Lu J, Wang Z, Cao J, Chen Y, Dong Y. A novel and compact review on the role of oxidative stress in female reproduction. *Reprod Biol Endocrinol* 2018;**16**:80
6. Al-Gubory KH, Fowler PA, Garrel C. The roles of cellular reactive oxygen species, oxidative stress and antioxidants in pregnancy outcomes. *Int J Biochem Cell Biol* 2010;**42**:1634–50
7. Kedzierska M, Olas B, Wachowicz B, Jeziorski A, Piekarski J. Relationship between thiol, tyrosine nitration and carbonyl formation as biomarkers of oxidative stress and changes of hemostatic function of plasma from breast cancer patients before surgery. *Clin Biochem* 2012;**45**:231–6
8. Singh M, Kasna S, Roy S, Aldosary S, Saeedan AS, Ansari MN, Kaithwas G. Repurposing mechanistic insight of PDE-5 inhibitor in cancer chemoprevention through mitochondrial-oxidative stress intervention and blockade of DuCLOX signalling. *BMC Cancer* 2019;**19**:996
9. Sun YW, Herzog CR, Krzeminski J, Amin S, Perdew G, El-Bayoumy K. Effects of the environmental mammary carcinogen 6-nitrochrysene on p53 and p21(Cip1) protein expression and cell cycle regulation in MCF-7 and MCF-10A cells. *Chem Biol Interact* 2007;**170**:31–9
10. Nandakumar R, Salini K, Devaraj SN. Morin accelerates proliferative inhibition via NF-jB mediated transcriptional regulation of apoptotic events during chemical carcinogen induced mammary cancer in rats. *Biomed Prev Nutr* 2014;**48**:277–90
11. Rajakumar T, Pugalendhi P, Thilagavathi S. Dose response chemopreventive potential of allyl isothiocyanate against 7,12-dimethylbenz(a) anthracene induced mammary carcinogenesis in female Sprague-Dawley rats. *Chem Biol Interact* 2015;**231**:35–43
12. El-Ghani MM. Traditional medicinal plants of Nigeria: an overview. *Agric Biol J N Am* 2016;**7**:220–47
13. Orishadipe AT, Okogun JI, Mishelia E. Gas chromatography-mass spectrometry analysis of the hexane extract of *Calliandra portoricensis* and its antimicrobial activity. *Afr J Pure Appl Chem* 2010;**4**:131–4
14. Ofusori DA, Adejuwon AO. Histopathological studies of acute and chronic effects of *Calliandra portoricensis* leaf extract on the stomach and pancreas of adult Swiss albino mice. *Asian Pac J Trop Biomed* 2011;**1**:182–5
15. Ogbole OO, Ndabai NC, Akinleye TE, Attah AF. Evaluation of peptide-rich root extracts of *Calliandria portoriscensis* (jacq.) Benth (Mimosaceae) for in vitro antimicrobial activity and brine shrimp lethality. *BMC Complement Med Ther* 2020;**20**:30
16. Moron MS, Depierre JW, Mannervik B. Levels of glutathione, glutathione reductase and glutathione S-transferase activities in rat lung and liver. *Biochim Biophys Acta* 1979;**582**:67–78
17. Enwuru V, Ogbonnia S, Mbaka G, Emordi J, Ota D, Onyebuchi P. Evaluation of histomorphological, toxicological and antimicrobial activities of ethanolic extract of *Calliandra portoricensis* root in rodents. *JPRI* 2017;**18**:1–13
18. Adaramoye O, Erguen B, Oyebode O, Nitzsche B, Höpfner M, Jung K, Rabien A. Antioxidant, antiangiogenic and antiproliferative activities of root methanol extract of *Calliandra portoricensis* in human prostate cancer cells. *J Integr Med* 2015;**13**:185–93
19. Siemuri EO, Akintunde JK, Salemcity AJ. Effects of Sub-acute methanol extract treatment of *Calliandra portoricensis* root bark on antioxidant

defence capacity in an experimental rat model. *J Basic Clin Physiol Pharmacol* 2015;**26**:375–82

20. Oyebode OT, Owumi SE, Oyelere AK, Olorunsogo OO. *Calliandra portoricensis* benth exhibits anticancer effects via alteration of bax/bcl-2 ratio and growth arrest in prostate LNCaP cells. *J Ethnopharmacol* 2019;**233**:64–72

21. Kinoshita Y, Yoshizawa K, Hamazaki K, Emoto Y, Yuri T, Yuki M, Kawashima H, Shikata N, Tsubura A. Dietary effects of mead acid on N-methyl-N-nitrosourea-induced mammary cancers in female Sprague-Dawley rats. *Biomed Rep* 2016;**4**:33–9

22. Keiler AM, Macejova D, Dietz BM, Bolton JL, Pauli GF, Chen SN, van Breemen RB, Nikolic D, Goerl F, Muders MH, Zierau O, Vollmer G. Evaluation of estrogenic potency of a standardized hops extract on mammary gland biology and on MNU-induced mammary tumor growth in rats. *J Steroid Biochem Mol Biol* 2017;**174**:234–41

23. Lim J, Ortiz L, Nakamura BN, Hoang YD, Banuelos J, Flores VN, Chan JY, Luderer U. Effects of deletion of the transcription factor Nrf2 and benzo [a]pyrene treatment on ovarian follicles and ovarian surface epithelial cells in mice. *Reprod Toxicol* 2015;**58**:24–32

24. Adefisan A, Owumi S, Adaramoye O. Root bark extract of *Calliandra portoricensis* (jacq.) benth. chemoprevents N-methyl-N-nitrosourea-induced mammary gland toxicity in rats. *J Ethnopharmacol* 2019;**233**:22–33

25. Lowry OH, Rosebrough NJ, Farr AL, Randall RJ. Protein measurement with the folin phenol reagent. *J Biol Chem* 1951;**193**:265–75

26. McCord JM, Fridovich I. Superoxide dismutase. An enzymic function for erythrocuprein (hemocuprein). *J Biol Chem* 1969;**244**:6049–55

27. Aebi H. Catalase estimation. In: *Methods of enzymatic analysis*. New York, NY: Verlag Chemic, 1974.

28. Habig WH, Pabst MJ, Jakoby WB. Glutathione S-transferases. The first enzymatic step in mercapturic acid formation. *J Biol Chem* 1974;**249**:7130–9

29. Rotruck JT, Pope AL, Ganther HE, Swanson AB, Hafeman DG, Hoekstra WG. Selenium: biochemical role as a component of glutathione peroxidase. *Science* 1973;**179**:588–90

30. Trush MA, Egner PA, Kensler TW. Myeloperoxidase as a biomarker of skin irritation and inflammation. *Food Chem Toxicol* 1994;**32**:143–7

31. Palmer RM, Ferrige AG, Moncada S. Nitric oxide release accounts for the biological activity of endothelium-derived relaxing factor. *Nature* 1987;**327**:524–6

32. Ellman GL. Tissue sulfhydryl groups. *Arch Biochem Biophys* 1959;**82**:70–7

33. Buege JA, Aust SD. Microsomal lipid peroxidation. *Methods Enzymol* 1978;**52**:302–10

34. Bancroft JD, Gamble M. *Theory and practice of histological techniques*. 6th ed. Beijing: Churchill Livingston/Elsevier, 2008.

35. Chakravarthi SL, Hannien AS, Pasupati B, Palayan T, Talib KA. The expression of p53 as a reliable immunohistochemical marker of gastric adenocarcinomas. *Res J Med Sci* 2010;**4**:15–9

36. Khadyrov EA, McHedlishvili M. [Specific features of neovascularization of dysplastic invasiveness and cancer of the breast]. *Georgian Med News* 2007;**142**:60–3

37. Sun Y. Free radicals, antioxidant enzymes, and carcinogenesis. *Free Radic Biol Med* 1990;**8**:583–99

38. Banerjee BD, Seth V, Bhattacharya A, Pasha ST, Chakraborty AK. Biochemical effects of some pesticides on lipid peroxidation and free-radical scavengers. *Toxicol Lett* 1999;**107**:33–47

39. Owumi SE, Nwozo SO, Effiong ME, Najophe ES. Gallic acid and omega-3 fatty acids decrease inflammatory and oxidative stress in manganese-treated rats. *Exp Biol Med* 2020;**245**:835–44

40. Arivazhagan L, Sorimuthu Pillai S. Tangeretin, a citrus pentamethoxyflavone, exerts cytostatic effect via p53/p21 up-regulation and suppresses metastasis in 7,12-dimethylbenz(alpha)anthracene-induced rat mammary carcinoma. *J Nutr Biochem* 2014;**25**:1140–53

41. Mansour SA, Mossa Abdel-Tawab H. Oxidative damage, biochemical and histopathological alterations in rats exposed to chlorpyrifos and the antioxidant role of zinc. *Pestic Biochem Phys* 2010;**96**:14–23

42. Akanni OO, Owumi SE, Olowofela OG, Adeyanju AA, Abiola OJ, Adaramoye OA. Protocatechuic acid ameliorates testosterone-induced benign prostatic hyperplasia through the regulation of inflammation and oxidative stress in castrated rats. *J Biochem Mol Toxicol* 2020; e22502. doi.10.1002/jbt.22502

43. Lowe SW, Cepero E, Evan G. Intrinsic tumour suppression. *Nature* 2004;**432**:307–15

44. Bitomsky N, Hofmann TG. Apoptosis and autophagy: regulation of apoptosis by DNA damage signalling – roles of p53, p73 and HIPK2. *FEBS J* 2009;**276**:6074–83

45. Loughery J, Cox M, Smith LM, Meek DW. Critical role for p53-serine 15 phosphorylation in stimulating transactivation at p53-responsive promoters. *Nucleic Acids Res* 2014;**42**:7666–80

46. Riley T, Sontag E, Chen P, Levine A. Transcriptional control of human p53-regulated genes. *Nat Rev Mol Cell Biol* 2008;**9**:402–12

47. Lin SQ, Jia FJ, Zhang CY, Liu FY, Ma JH, Han Z, Xie WD, Li X. Actinomycin V suppresses human non-small-cell lung carcinoma A549 cells by inducing G2/M phase arrest and apoptosis via the p53-dependent pathway. *Mar Drugs* 2019;**17**:572

48. Lakshmi A, Subramanian SP. Tangeretin ameliorates oxidative stress in the renal tissues of rats with experimental breast cancer induced by 7,12-dimethylbenz[a]anthracene. *Toxicol Lett* 2014;**229**:333–48

49. Abolaji AO, Ojo M, Afolabi TT, Arowoogun MD, Nwawolor D, Farombi EO. Protective properties of 6-gingerol-rich fraction from *Zingiber ofcinale* (ginger) on chlorpyrifos-induced oxidative damage and inflammation in the brain, ovary and uterus of rats. *Chem Biol Interact* 2017;**270**:15–23

50. Adaramoye O, Erguen B, Oyebode O, Nitzsche B, Hopfner M, Jung K, Rabien A. Antioxidant, antiangiogenic and antiproliferative activities of root methanol extract of *Calliandra portoricensis* in human prostate cancer cells. *J Integr Med* 2015;**13**:185–93

51. Liang Y, Mafuvadze B, Besch-Williford C, Hyder SM. A combination of p53-activating APR-246 and phosphatidylserine-targeting antibody potently inhibits tumor development in hormone-dependent mutant p53-expressing breast cancer xenografts. *Breast Cancer* 2018;**10**:53–67

52. Reed SM, Quelle DE. p53 acetylation: regulation and consequences. *Cancers* 2014;**7**:30–69

53. Yuri T, Lai YC, Yoshizawa K, Tsubura A. Human chorionic gonadotropin inhibits N-methyl-N-nitrosourea-induced mammary carcinoma growth in female Lewis rats. *In Vivo* 2012;**26**:361–7

54. Gehring C, Siepmann T, Heidegger H, Jeschke U. The controversial role of human chorionic gonadotropin in the development of breast cancer and other types of tumors. *Breast* 2016;**26**:135–40